Flow Patterns of Liquid in a Cylindrical Mixing Vessel without Baffles

AUTHOR(S):

NAGATA, Shinji; YAMAMOTO, Kazuo; UJIHARA, Motohiro

CITATION:

NAGATA, Shinji ...[et al]. Flow Patterns of Liquid in a Cylindrical Mixing Vessel without Baffles. Memoirs of the Faculty of Engineering, Kyoto University 1958, 20(4): 336-349

ISSUE DATE:

1958-12-01

URL:

http://hdl.handle.net/2433/280423

Flow Patterns of Liquid in a Cylindrical Mixing Vessel without Baffles

By

Shinji NAGATA, Kazuo YAMAMOTO and Motohiro UJIHARA

Department of Chemical Engineering

(Received August 22, 1958)

Abstract

The velocity distribution of agitated liquid in a cylindrical mixing vessel was measured by using a set of pitot tubes, the construction of which is shown in **Fig. 2.**

Some of the experimental results are shown in **Figs. 4, 5, 6, 7, 8, 9** and **10.**

As a result, the flow patterns in an agitated vessel were made clear and it was ascertained that, in addition to the primary circulation flow around the impeller axis, there was a secondary circulation of liquid ensued by the discharge flow from the tip of an impeller as shown in **Figs. 8** and **10.** Integrating the measured velocity distributions, the discharge flow rates of impellers were determined and the discharging performance of various impellers (refer to **Table 1**) was compared in connection with the power consumption. Dimensionless factor, N_{q1}, was defined and was called the coefficient of discharge. The ratio, N_P/N_{q1} in **Table 3,** corresponds to the relative power required for a unit quantity of discharge.

Furthermore, the power consumption in the neighbourhood of an impeller (N_{Pimp}), in other words, in the cylindrical domain (refer to hatched region in **Fig. 14**) was calculated and compared with that consumed in the outer region of the vessel as shown in **Table 4.**

It is concluded that the improvement in the discharging capacity can be accomplished to some extent by the proper design of an impeller; however, the fundamental improvement must rely upon some other method.

1. Equipment used and method of measurement

1) Pitot tubes.

As the flow pattern of liquid in a cylindrical mixing vessel is three dimensional, the direction and velocity of flow should be measured. By measuring the angles θ and φ in **Fig. 1,** three dimensional directions of flow are determined. As shown in

the diagram, the angle θ shows a horizontal direction of flow and is given a positive or negative sign depending upon the stream which is either outwards or inwards against the tangent of the circle which passes through the point of interest. Also, the angle φ shows the vertical direction and is given a positive or negative sign depending upon the stream which is either upwards or downwards against the horizontal plane.

The pitot tubes used for the measurement of θ and φ are composed of two parrallel connected pipes as shown in **Fig. 2,** the tips of which are cut to a sharp angle as shown in the diagram. When both the directions of the pitot tube and of liquid flow are consistent, the readings of both columns of the manometer are also consistent. The pitot tube (**a**) can be rotated around its axis and is used for measuring the angle θ. The second one (**b**) can be rotated along the vertical plane and is used for measuring the angle φ. Both of them are so arranged that their tips are always fixed to one point (point of measurement) regardless of the angle they are turned.

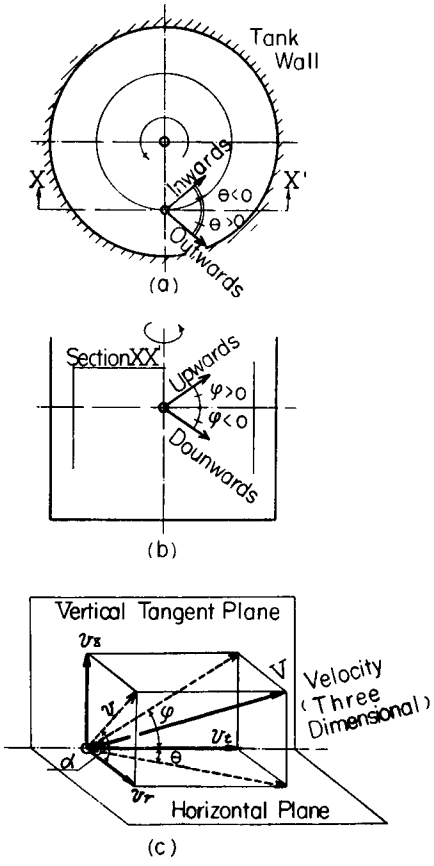

Fig. 1. Measurement of Flow Direction.

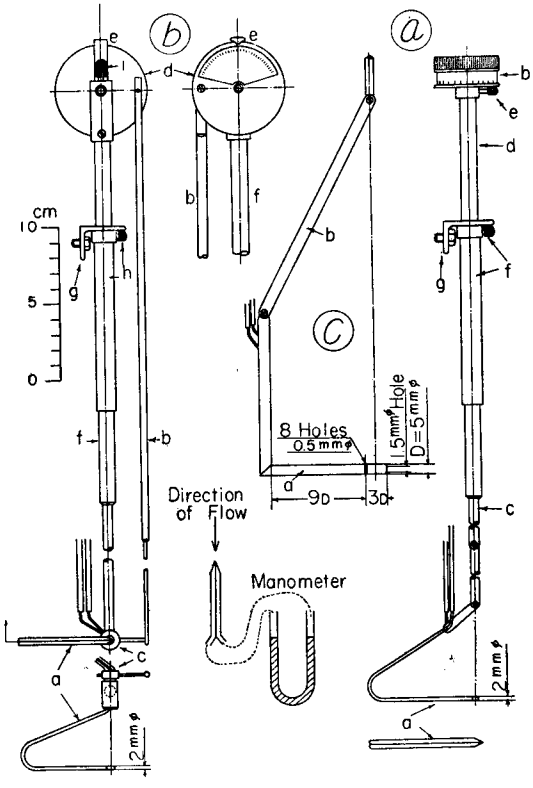

Fig. 2. Construction of Pitot Tubes.

After the direction of flow is determined, the liquid velocity is measured by inserting a pitot tube of Prandtl type (**c**). The deviation of manometer readings due to discrepancy between the direction of flow and the axis of the pitot tube is so small in this Prandtl type that the deviations of $\pm 10°$ in their angles of direction have little effect on the results of observation. The arrngement of this pitot tube is shown in **Fig. 2** (**c**), the upper part of which is similar to that of (**a**).

The pitot tubes for θ and φ have a sensitivity of 1 mm water column pressure difference corresponding to the deviation of 1° when the liquid velocity is 60 cm/sec. The velocity coefficient of the pitot tube of Prandtl type was 0.99 in the range of application.

2) Impellers and vessel.

The impellers used are shown in **Table 1** and the conditions of their installation are shown in **Fig. 3.** The vessel used has a diameter of 58.5 cm and is filled with the tap water to the depth equal to the diameter. The impellers are always installed at one half of the water depth and the distance between this point and the water level is measured and this is marked z. The radial distance is measured from the central impeller axis and is marked r.

Almost all of the impellers used had numerous blades (mostly eight blades); therefore, excepting a few cases of special impellers, the flow patterns in an agitated vessel were considered to have axial symmetry and, also, a plane symmetry in reference to the rotation plane of impellers. Therefore, it was sufficient to measure the flow pattern within the hatched area shown in **Fig. 3.**

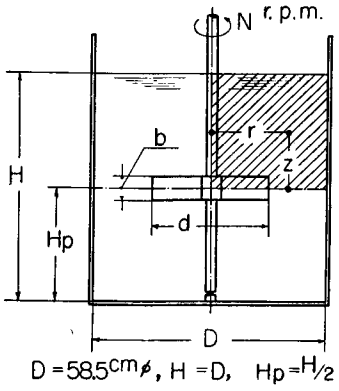

Fig. 3. Schematic Dingram of Impeller and Vessel.

3) Method of calculation of the three components of liquid velocity.

The three components of liquid velocity, i.e., (1) tangential velocity (v_t), (2) radial velocity (v_r) and (3) axial velocity (v_z) are shown in **Fig. 1** (**c**) and these are calculated from the values of θ, φ and V by using the following equations.

$$\left.\begin{aligned} v_t &= \frac{V}{\sqrt{1+\tan^2\theta+\tan^2\varphi}} \\ v_r &= \frac{V}{\sqrt{1+\tan^2\theta+\tan^2\varphi}} \cdot \tan\theta \\ v_z &= \frac{V}{\sqrt{1+\tan^2\theta+\tan^2\varphi}} \cdot \tan\varphi \end{aligned}\right\} \qquad (1)$$

Table 1. Various Types of Impellers used.
(dimensions in cm)

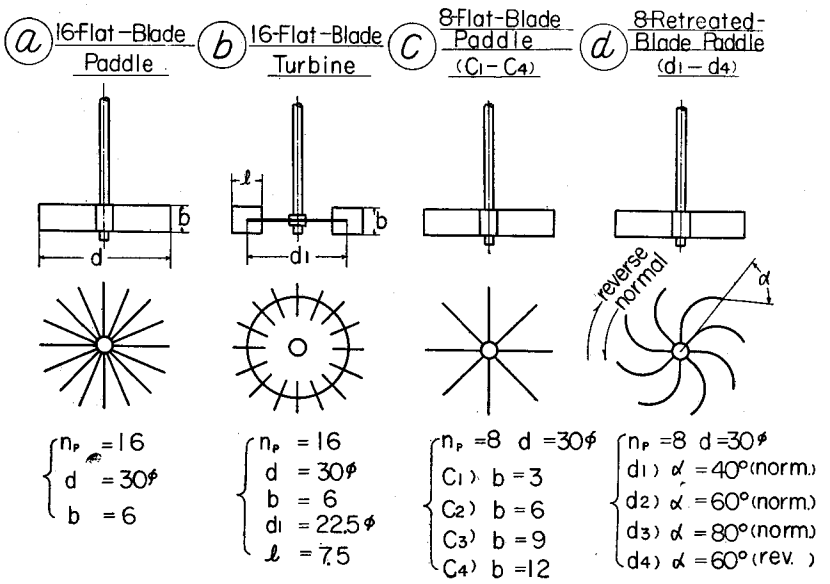

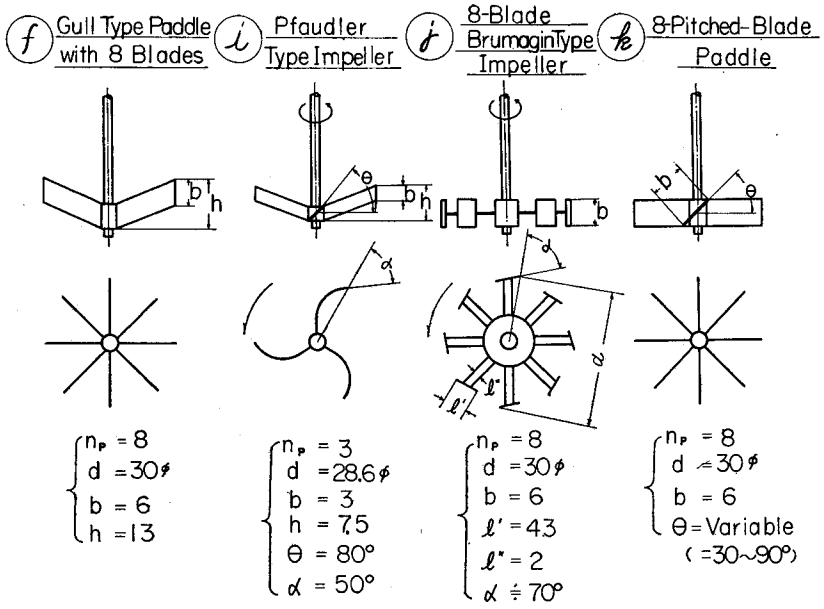

As regards the axially symmetrical flow, the flow patterns in the $r-z$ plane can be drawn similarly as in the case of two dimensional flow. In this case, the resultant velocity v on that plane and the angle α between the direction of v and the horizontal plane can be calculated from the following equations (refer to **Fig. 1 (c)**).

$$\left.\begin{aligned} v &= \frac{\sqrt{\tan^2\varphi+\tan^2\theta}}{\sqrt{1+\tan^2\theta+\tan^2\varphi}}\cdot V \\ \alpha &= \tan^{-1}\left(\frac{\tan\varphi}{\tan\theta}\right) \end{aligned}\right\} \quad (2)$$

2. Results obtained

As typical examples of θ, φ and V, the data obtained in the case of 16-blade paddle (refer to **Table 1 (a)**) are shown in **Fig. 4, 5** and **6.** In **Fig. 4,** the distribution of the angle θ in various heights is drawn for several radial positions. In **Fig. 5,** the distribution of the angle φ in various radial positions is drawn for several horizontal levels. In **Fig. 6,** the resultant velocity distribution (V) in various radial positions is drawn for several horizontal levels. From these data, three components of liquid velocities v_t, v_r and v_z can be calculated by using Eq. (1). **Fig. 7, 8** and **9** are drawn from these procedures.

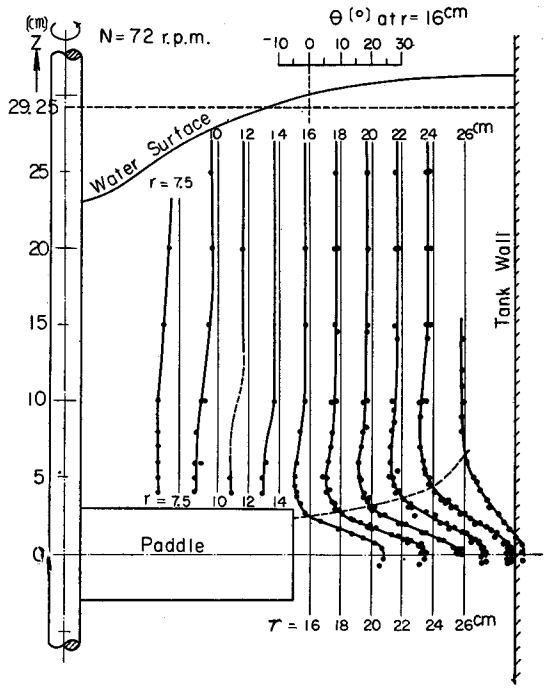

Fig. 4. Distribution of θ for 16-Flat-Blade Paddle.

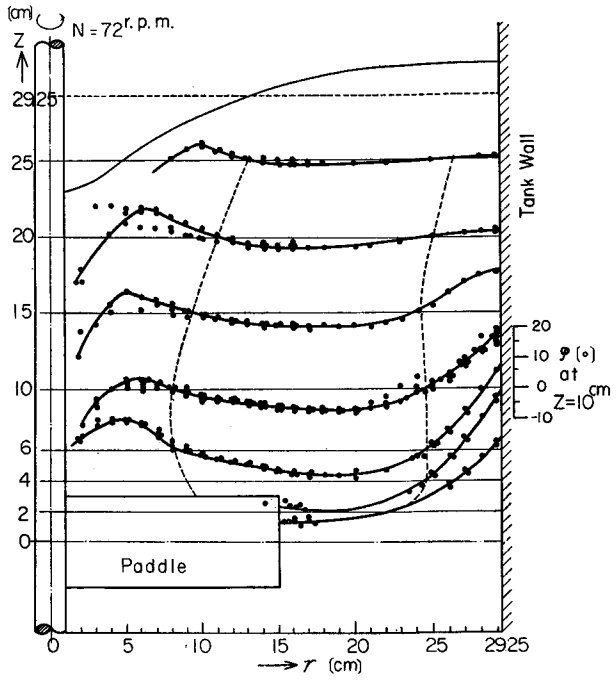

Fig. 5. Distribution of φ for 16-Flat-Blade Paddle.

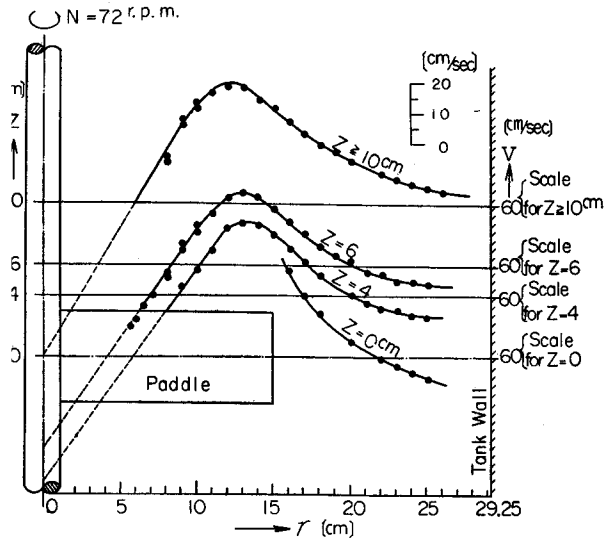

Fig. 6. Distribution of V for 16-Flat-Blade Paddle.

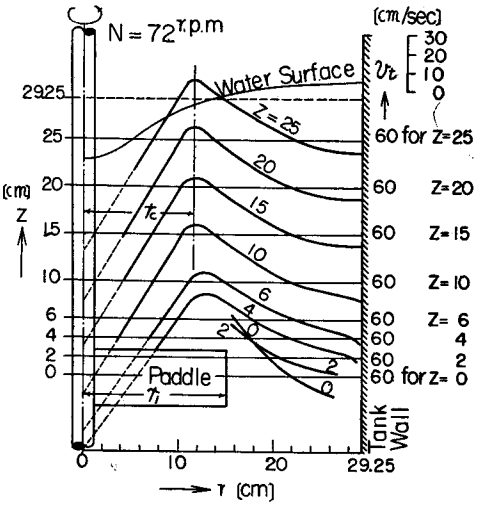

Fig. 7. Distribution of tangential velocity (v_t).

As shown in **Fig. 7,** the tangential velocity v_t is approximately proportional to the radial distance (r) in the central zone. This region is called the cylindrical rotating zone. Outside of this region, there appears a quasi-potential flow which is shown in this figure.

The radius of the cylindrical rotating zone (r_c) is a little larger in the vicinity of the impeller, and nears the constant value in the region 10 cm or more apart from the impeller ($z \geqq 10$ cm) and the flow pattern becomes similar.

The radius (r_c) and the angular velocity of cylindrical rotating zone vary more or less in accordance with the type of impellers and also with the impeller speed as will be referred to later. In the present case, the value of r_c is equal to 80% of the impeller radius (r_1) and the angular velocity of liquid is approximately 10% higher than the impeller velocity.

This phenomenon seems to be due to the secondary circulation flow; in other words, the angular momentum of the discharging flow from the tips of impeller blades is transmitted to this cylindrical rotating zone and thus accounts for this increment.

The distribution of the radial velocity component (v_r) is shown in **Fig. 8.** As shown in this diagram, there is a radial flow ($F_1F_0F_1'$) discharged outwards from the impeller and also a suction flow ($F_1F_2F_3$) towards the impeller at the upper level.

The distribution of the axial flow (v_z) is shown in **Fig. 9.** As shown in this diagram, there is an upward current ($F_0F_1F_0'$) in the neighbourhood of the vessel wall especially in the range of small z values; and in the inside region, there is a downward flow ($F_1F_2F_3$) sucked towards the impeller.

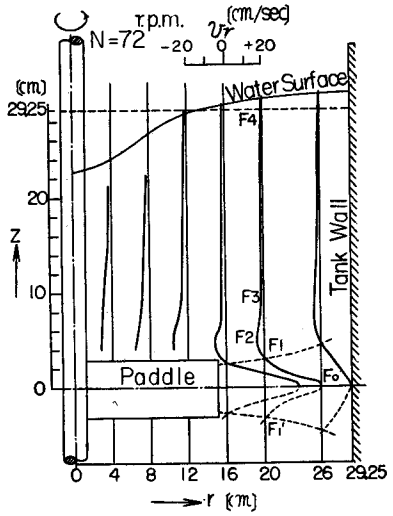

Fig. 8. Distribution of radial velocity (v_r).

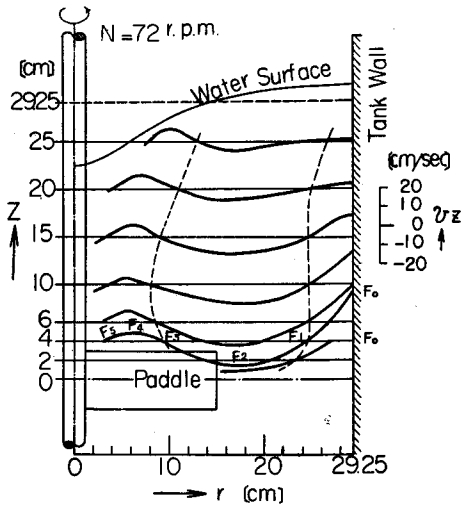

Fig. 9. Distribution of axial velocity (v_z).

In summary, there is a secondary circulation flow which is at first discharged from the impeller against the vessel wall, hits against it, ascends along it, and then returns to the impeller in the central region of the vessel. **Fig. 10** is a schematic diagram of this secondary circulation flow in the $r-z$ plane shown as a two-dimensional flow. As shown in this diagram, the discharge flow sucks in certain amount of liquid from the upper region and increases its flow volume. After changing its direction in the upper zone of the vessel, the secondary circulation flow, as given above, descends along the inner region. A part of this downward flow joins the discharge flow (refer to Fig. 10 curve 1, 2, 3 and 4), while the rest is sucked further towards the impeller and once again thrown out as a discharge flow (refer to curve 5, 6 and 7). The point V in the diagram is the center of the secondary circulation flow.

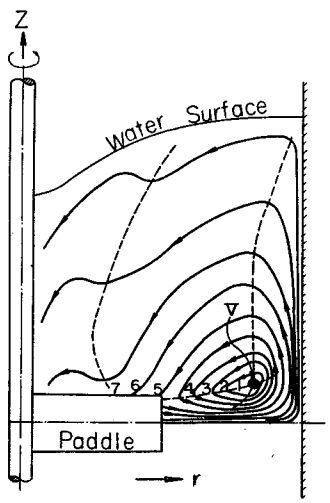

Fig. 10. Flow Pattern of Secondary Circulation Flow.

Since the flow patterns are similar with all impellers (refer to **Table 1**), other diagrams are omitted and only the data derived from those diagrams referred to the following sections.

3. Comparison of the results obtained

1) Comparison of the flow distributions.

The qualitative trends of the velocity distribution are similar with all types of impellers, but there are noteworthy differences in a few types of them.

The distribution of v_t with the change of r and that of v_r with the change of z are shown in **Fig. 11 a, b** and **Fig. 12 a, b.**

Comparisons of the results obtained between 8-flat-blade paddle (c_2), 8-curved-blade paddle (d_1) and 8-pitched-blade paddle (k) are shown in **Fig. 11 a** and **b.** As mentioned above, the velocity distribution at the distance over 10 cm from the impeller ($z \geqq 10$ cm) is almost constant, the distribution of v_t at $z=13$ cm is shown in part **a.** From this diagram, it is evident that the curved-blade or pitched-blade impeller tends to give a smaller tangential velocity (v_t) and a smaller radius of r_c than the flat blade impellers.

On the other hand, the width of the discharging flow is increased and it gives a larger volume of flow as shown in part **b.** As for the pitched-blade impeller, the discharging flow is shifted upwards (or downwards) and loses its similarity to the rotation plane of the impeller.

Similar comparisons were made on the 8-blade paddles having various widths but equal diameter,

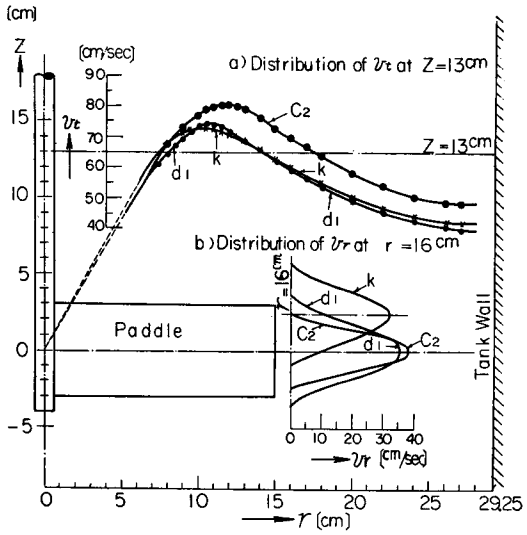

Fig. 11. Velocity Distribution of Various Types of Impellers.

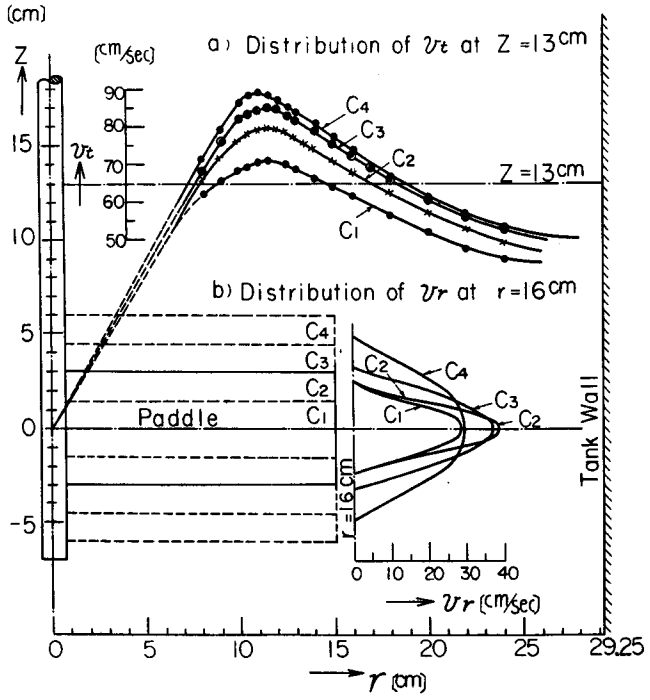

Fig. 12. Velocity Distribution of Various Types of Impellers.

and the results obtained are shown in **Fig. 12 a** and **b.** By increasing the width of blades, both the tangential and discharging velocities increase remarkably. In the case of the flat-blade paddles, the total width of the blade does not contribute to the discharging flow, but a suction flow is seen at the corners of the blades. This trend is not shown in the case of the impellers having curved or pitched blades, and the results are obtained as if the blade widths were increased.

2) Discharging flow and the efficiency of impellers.

As stated above, there is a primary circulation flow around the impeller axis and, on the other hand, there is also a secondary circulation flow caused by the discharging liquid. For simplicity, let us assume a case in which these flows are completely symmetric in reference to the impeller axis and the horizontal rotation plane.

The primary circulation flow q_0 around an impeller axis is expressed by the following equation:

$$q_0 = \int_{-H/2}^{H/2} \int_0^{D/2} v_t \, dr \, dz \,. \tag{3}$$

Now, let us assume a cylindrical boundary surface whose radius and height are equal to r_s and $2z_s$ respectively with an impeller in the middle as shown in **Fig. 13.** Then the volume of the discharging flow, q_1 and of the secondary circulation flow, q_2 can be expressed as follows:

$$q_1 = 4\pi r_s \int_0^{z_p} v_r \, dZ \tag{4}$$

$$q_2 = 4\pi \int_{r_0}^{D/2} v_z \, r \, dr \,. \tag{5}$$

The volume, q_3, which comes back from the outside and is sucked towards the impeller, is:

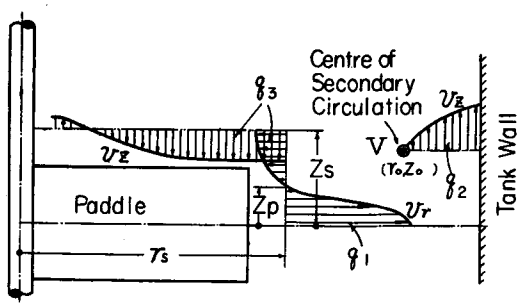

Fig. 13. Cylindrical Boundary surface taken considering the energy dissipation.

$$q_3 = 4\pi \left\{ r_s \int_{z_p}^{z_s} v_r dZ + \int_0^{r_s} v_z \, r \, dr \right\} = q_1 \,. \tag{6}$$

Therefore, the portion of the liquid q_4 which is sucked in from the upper and the lower regions of the discharge flow is equal to $q_2 - q_1$:

$$q_4 = q_2 - q_1 \,. \tag{7}$$

Equally, the quantity of flow can be calculated at any given surface. Consequently, under the same conditions as shown in **Fig. 4,** i.e., with 16-blade impeller at 72 r.p.m., the secondary circulation flow can be drawn quantitatively as shown in **Fig. 14.**

In the upper half of the vessel, approximately 5.3 l/sec ($q_1/2$) of water is discharged from the tip of the impeller and approximately 4.2 l/sec ($q_4/2$) of water is concurrently drawn into it from the upper zone, and the confluent of 9.5 l/sec ($q_2/2$) forms the secondary circulation flow. Summing up the upper and lower half of the vessel, q_2 amounts to 19 l/sec. In comparison with this, the primary circulation flow q_0 becomes nearly equal to 110 l/sec. Thus, the secondary circulation flow is comparatively small, but it is very important because it contributes to the mixing of the water in the vertical direction.

As these quantities of circulation q_1 and q_2 change at different impeller speeds, it is advisable to use a dimensionless group for generalization, thus:

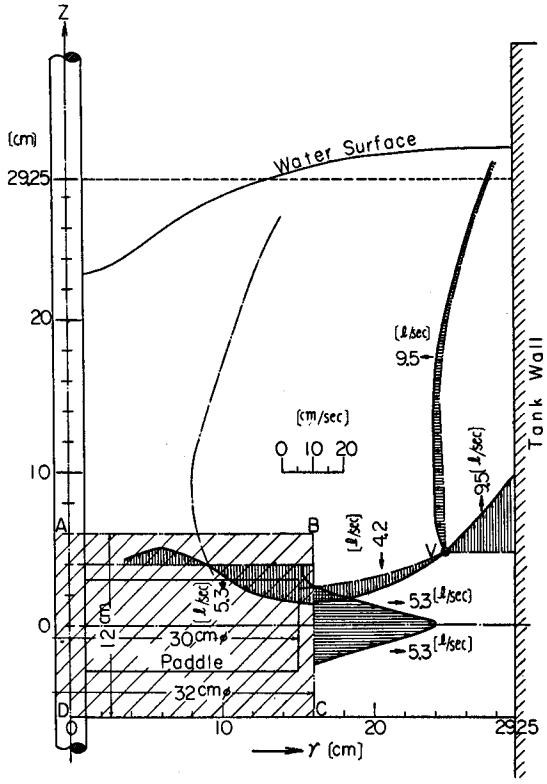

Fig. 14. Schematic diagram of secondary circulation flow (16-flat-blade paddle, 72 r.p.m.)

$$N_{q_1} = q_1/nd^3, \qquad N_{q_2} = q_2/nd^3. \tag{8}$$

In the above equations n is the impeller speed in r.p.s., d is the diameter of an impeller, and N_{q_1} and N_{q_2} are called the "coefficient of discharge" and "coefficient of secondary circulation" respectively. These values, as shown in **Table 2,** do not show any notable variation at different impeller speeds.

Now, for the purpose of comparison of discharging efficiency of various types

Table 2. Discharging Performance of 16-Flat-Blade Paddle (a).
d=30 cmϕ, b=6 cm, n_p=16,
D=58.5 cmϕ, H=D, H_p=$H/2$

N [r.p.m.]	q_1 [ltr/sec.]	q_2 [ltr/sec.]	q_2/q_1	N_{q1}	N_{q2}	N_P	N_P/N_{q1}	N_P/N_{q2}
38	6.1	11.0	1.80	0.36	0.64	1.12	3.1	1.8
72	10.6	18.9	1.78	0.33	0.58	1.08	3.3	1.9
100	13.3	28.8	2.17	0.30	0.64	1.04	3.5	1.6
132	16.8	32.2	1.92	0.27	0.52	0.99	3.7	1.9

of impellers, the ratio of the power number $N_P=(P\cdot g_c/\rho n^3 d^5)$ and the coefficient of discharge N_{q_1} is adopted:

$$\frac{N_P}{N_{q_1}}=\frac{P\cdot g_c}{\rho n^2 d^2\cdot q_1}. \tag{9}$$

When the impeller is considered as a sort of circulation pump, N_P/N_{q_1} is a ratio of power necessary for a constant circulation. Therefore, when this ratio is large, it means that the local turbulence is great and the circulation efficiency is low; and when this ratio is small, it means that the circulation efficiency is high. The results derived from the observed values are shown in **Table 3.**

Table 3. Discharging Performance of Various Impellers.

	Impeller	d/D	b/D	N_P	N_{q1}	N_P/N_{q1}	$\mathrm{Re}\times10^{-5}$
a	16-Flat-Blade Paddle	0.513	0.1026	1.08	0.33	3.3	1
b	16-Flat-Blade Turbine	〃	〃	1.06	0.33	3.2	〃
c_1	8-Flat-Blade Paddle	〃	0.0513	0.81	0.25	3.2	〃
c_2	〃	〃	0.1026	0.95	0.34	2.8	〃
c_3	〃	〃	0.154	1.04	0.47	2.2	〃
c_4	〃	〃	0.205	1.07	0.59	1.8	〃
d_1	8-Retreated-Blade Paddle	〃	0.1026	0.88	0.43	2.0	〃
d_2	〃	〃	〃	0.71	0.43	1.7	〃
d_3	〃	〃	〃	0.55	0.37	1.5	〃
d_4	〃	〃	〃	1.06	0.27	3.9	〃
e_1	8-Flat-Blade Paddle (2/3 of the corners are cutt off)	〃	〃	0.84	0.24	3.5	〃
e_2	〃 (1/4 〃 〃 〃 〃)	〃	0.205	1.05	0.51	2.1	〃
e_3	〃 (1/3 〃 〃 〃 〃)	〃	〃	1.04	0.46	2.3	〃
e_4	〃 (1/2 〃 〃 〃 〃)	〃	〃	0.99	0.46	2.2	–
l	〃 (Corners are widen)	〃	0.1026	1.09	0.46	2.4	〃
f	Gull Type Paddle with 8 Blades	〃	〃	0.94	0.28	3.4	〃
g	8-Blade-Arrow-Head Turbine	〃	〃	0.95	0.26	3.7	〃
h	3-Flat-Blade Paddle	0.489	0.0513	0.60	0.19	3.2	〃
i	Pfaudler Type Impeller	〃	〃	0.37	0.23	1.6	〃
j	8-Blade-Brumagin-Type Impeller	0.513	0.1026	0.44	0.34	1.3	〃
k	8-Pitched-Blade Paddle ($\theta=90°$)	〃	〃	0.95	0.34	2.8	〃
	〃 ($\theta=60°$)	〃	〃	0.84	0.36	2.3	〃
	〃 ($\theta=45°$)	〃	〃	0.72	0.31	2.3	〃
	〃 ($\theta=30°$)	〃	〃	0.51	0.30	1.7	〃
p_1	8-Flat-Blade Paddle	0.308	〃	2.17	1.23	1.8	0.37
c_2	〃	0.513	〃	0.95	0.34	2.8	1
o_2	〃	0.718	〃	0.57	0.144	4.0	2
q	Rotating Disc	0.513	—	0.045	0.031	1.45	2.1
	〃 (Theoretical Value)	〃	—	0.045_3	0.027_4	1.65	〃
	6-Flat-Blade Turbine[1] in Baffled Condition	0.348	0.0696	(7.5)	0.932	8.05	0.15～0.3

$N_P=P\cdot g_c/\rho n^3 d^5$, $N_{q1}=q_1/nd^3$, $\mathrm{Re}=nd^2/\nu$,

Referring to this table, the values of N_P/N_{q_1} vary greatly from 1.5 to 3.5 or more according to the types of impellers and they can be grouped into two main classes. When this ratio is large it is called the shearing type and when the ratio is small, it is called the circulation type.

In the turbulent region, there is little difference between the paddles and the flat-blade turbines from the standpoint of discharge; and the discharging efficiency can be improved by adopting a curved blade impeller (d), wide-blade impellers (c_3), (c_4) or a pitched-blade impeller (k). Also, a smaller impeller in comparison with the vessel diameter shows a similar effect (refer to **Table 3** (p_1)). Comparing the results of impellers c_2 vs e_1 and c_4 vs e_2, e_3, e_4, the effect of the corner of blades is revealed and it is found that elimination of the corners would decrease the secondary circulation flow.

In the bottom line of **Table 3,** the result obtained with the flat-blade turbine with baffle plates is shown which was measured by Sachs and Rushton[1] with photographic method. This result goes to show that the application of ordinary type of baffle plates is ineffective from the standpoint of circulation.

3) Energy balance in the neighbourhood of impellers.

The energy balances referring to the momentum transfer of liquid flow can be obtained just as the balance of flow quantity in the neighbourhood of the impeller was obtained. The amount of energy going out from the cylindrical domain near the impeller per unit time (P_0) (refer to **Fig. 14**) can be expressed as follows:

$$P_0 = \frac{\rho}{g_c} 2\pi r_s \int_0^{z_p} v_r V^2 dz + 4\pi r_s \int_0^{z_p} v_r p\, dz + \frac{\rho g}{g_c} 4\pi r_s \int_0^{z_p} v_r z\, dz \tag{10}$$

The amount of energy returning to an impeller per unit time from the cylindrical boundary (P_i) is:

$$\begin{aligned} P_i = {} & \frac{\rho}{g_c} 2\pi r_s \int_{z_p}^{z_s} v_r V^2 dz + 4\pi r_s \int_{z_p}^{z_s} v_r p\, dz + \frac{\rho g}{g_c} 4\pi r_s \int_{z_p}^{z_s} v_r z\, dz \\ & + \frac{\rho}{g_c} 2\pi \int_0^{r_s} v_z r V^2 dr + 4\pi \int_0^{r_s} v_z r p\, dr + \frac{\rho g}{g_c} 4\pi z_s \int_0^{r_c} v_z r\, dr \end{aligned} \tag{11}$$

Now, taking a cylindrical domain of 32 cm in diameter and 12 cm in height with an impeller in the center as shown in the hatched area in **Fig. 14,** the liquid volume of this domain corresponds to 6% of the total agitated liquid. Combining the input and output of the power values in this cylindrical domain, the followings are obtained:

$$N_P = \frac{\text{power consumption by impellers}}{\rho n^3 d^5/g_c} \tag{12}$$

$$N_{P_0} = \frac{\left[\begin{array}{l}\text{power transmitted to the outside region by discharging} \\ \text{flow from the inside of the cylindrical domain}\end{array}\right]}{\rho n^3 d^5/g_c} \tag{13}$$

$$N_{Pi} = \frac{\left[\begin{array}{l}\text{power returned to the inside region from the}\\ \text{outside of the cylindrical domain}\end{array}\right]}{\rho n^3 d^5/g_c} \tag{14}$$

$$\Delta N_P = N_{P0} - N_{Pi} = \frac{\left[\begin{array}{l}\text{power consumption by the liquid}\\ \text{outside the cylindrical domain}\end{array}\right]}{\rho n^3 d^5/g_c} \tag{15}$$

$$N_{Pimp} = N_P - \Delta N_P = \frac{\left[\begin{array}{l}\text{power consumption by the liquid}\\ \text{inside the cylindrical domain}\end{array}\right]}{\rho n^3 d^5/g_c} . \tag{16}$$

In reference to several impellers, these values are calculated and compared in **Table 4.** These data, however, are not very accurate, and contain errors of $\pm 10 \sim 20\%$.

Table 4. Energy Belance in the Neighbourhood of Impellers.
d=30 cmϕ, b=6 cm,
D=58.5 cmϕ, $H=D$, $H_p=H/2$

Impeller	N_P	N_{P0}	N_{Pi}	ΔN_P	N_{Pimp}	$\frac{N_{Pimp}}{N_P}\times 100$
(a) 16-Flat-Blade Paddle	1.08	2.5	2.3	0.2	0.88	81%
(c_2) 8-Flat-Blade Paddle	0.95	2.5	2.2	0.3	0.65	68%
(d_1) 8-Retreated-Blade Paddle	0.71	2.25	2.0	0.25	0.46	65%

In short, a greater part of the energy transferred to the liquid through the discharging flow returns to the impeller with the circulation of the flow and the difference between the outgoing and returning energy corresponds to the power consumed by the impeller. And more than one half of the power is consumed by the turbulence in the vicinity of the impeller. This trend cannot be improved appreciably by a mere modification of impeller blades. Therefore, from the standpoint of convective circulation of liquid, the efficiency of mixing impellers can be said very low.

Acknowledgment

The authors wish to express their heartiest appreciation to the Shinko Pfaudler Company Ltd. which was kind enough to furnish them with the pitot tubes and some of the impellers used in this study.

Nomenclature

b	:	Width of impeller blades	[cm]
D	:	Tank diameter	[cm]
d	:	Impeller diameter	[cm]
g_c	:	Gravitational conversion factor	[g·cm/G·sec^2]
H	:	Liquid depth	[cm]

H_p : Height of impeller from the tank bottom [cm]

$N_P = P \cdot g_c / \rho n^3 d^5$: Power number [−]

$N_{q_1} = q_1 / n d^3$: Coefficient of discharge [−]

$N_{q_2} = q_2 / n d^3$: Coefficient of secondary circulation [−]

N_{P_0} =[Power trasmitted to the outside region by discharging flow from the inside of the boundary surface as shown in Fig. 14] $\div [\rho n^3 d^5 / g_c]$ [−]

N_{P_i} =[Power returned to the inside region from the outside of the boundary surface as shown in Fig. 14] $\div [\rho n^3 d^5 / g_c]$ [−]

$\Delta N_P = N_{P_0} - N_{P_i}$ =[Power consumption by the liquid outside the boundary surface as shown in Fig. 14] $\div [\rho n^3 d^5 / g_c]$ [−]

$N_{P_{imp}} = N_P - \Delta N_P$ =[Power consumption by the liquid inside the boundary surface as shown in Fig. 14 (i.e. Power consumption in the neighbourhood of an impeller)] $\div [\rho n^3 d^5 / g_c]$ [−]

N : Impeller speed in r.p.m. [1/min]

n : Impeller speed in r.p.s. [1/sec]

n_p : Number of impeller blades [−]

P : Power consumption of impellers [G·cm/sec]

p : Static pressure in liquid [G/cm²]

q_0 : Flow rate due to the circulation about an agitator axis (primary circulation) [c.c./sec] or [liter/sec]

q_1 : Discharge flow rate from the tip of impeller blades [c.c./sec] or [liter/sec]

q_2 : Flow rate due to secondary circulation [c.c./sec] or [liter/sec]

$q_3 = q_1$: Suction flow rate of an impeller [c.c./sec] or [liter/sec]

$q_4 = q_2 - q_1$: Induced flow rate caused by the discharge flow [c.c./sec] or [liter/sec]

r : Radial position from an agitator axis [cm]

V : Resultant velocity of liquid [cm/sec]

v_t : Circumferential component of liquid velocity [cm/sec]

v_r : Radial component of liquid velocity [cm/sec]

v_z : Vertical component of liquid velocity [cm/sec]

z : Height from the middle of liquid depth [cm]

α, θ, φ : Angles determining the flow direction (refer to Fig. 1 (c)) [−]

References

1) Sachs, J. P. & Rushton, J. H.: Chem. Eng. Prog. Vol. 50, p. 597 (1954).